

UHV-IR spectroscopy study of carbon monoxide adsorption on cerium oxide surfaces

Chengwu Yang,^{1,2} Fabian Bebensee,¹ Alexei Nefedov,¹ Christof Wöll^{1,2}

Infrared Reflection Absorption Spectroscopy (IRRAS) of Adsorbates on Metal Oxides

Introduction

Redox reactions stand an important place in chemical reactions in general and catalysis in particular. One of the most important materials in heterogeneous catalysis for this type of reaction is ceria. As a result of the fairly low energy needed to create oxygen vacancies at the surface of this material, it is often referred to as one of the most easily reducible materials. There are numerous applications of this unique rare-earth metal oxide ranging from heterogeneous catalysis, such as in vehicle emission control, to ethanol steam reforming and water gas shift reactions. In these cases, the oxidation reduction cycle ($\text{Ce}^{4+}/\text{Ce}^{3+}$ cations and the associated oxygen vacancies) is the most determining factor.

Here we used a novel apparatus combining a state-of-the-art FTIR spectrometer with a dedicated UHV-chamber to monitor the adsorption of CO on CeO_2 surfaces. The system allows acquiring both reflection spectra at grazing incidence on single crystals and transmission spectra on polycrystalline powders.^{1,2} CO is one of the most convenient probe molecule, and typically the CO stretch frequency shows substantial variations upon changes in the charge state of the metal ion the CO is bound to.

In the present study,³ we first determined the stretch frequency of CO adsorbed on a pristine single crystalline $\text{CeO}_2(111)$ surface using infrared reflection absorption spectroscopy (IRRAS). These results alone allow to correct previous assignments of IR-bands observed for CO adsorbed on ceria powder. Then, we deliberately introduced oxygen vacancies on the $\text{CeO}_2(111)$ surface. We clearly detected the presence of a new species with blue shift of around 10 cm^{-1} in the stretch frequency. By combining our experimental findings with first-principles density functional theory (DFT) calculations, we are able to propose an assignment for the slightly higher CO stretch frequency. These findings demonstrate that, on oxide surfaces, geometric effects can be more important for weak chemical interactions with surface cations than their (formal) charge state.

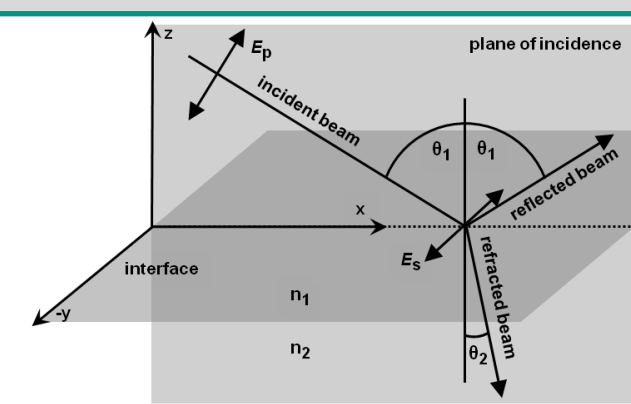


Figure 1. Beam geometry and polarization of IR radiation at the interface between two optically different media.⁴

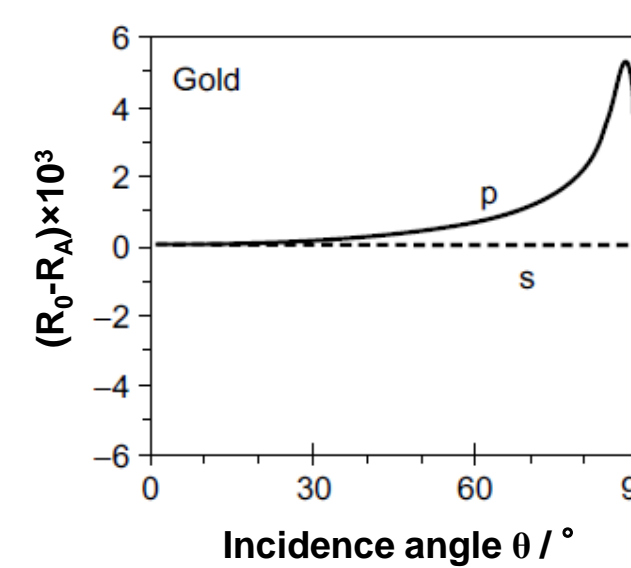


Figure 2. Calculated reflectivity differences between the clean gold (R_0) and the adsorbate-covered gold (R_A) as a function of incidence angle for p -polarized light (solid line) and s -polarized light (dashed line) at 3000 cm^{-1} .⁴

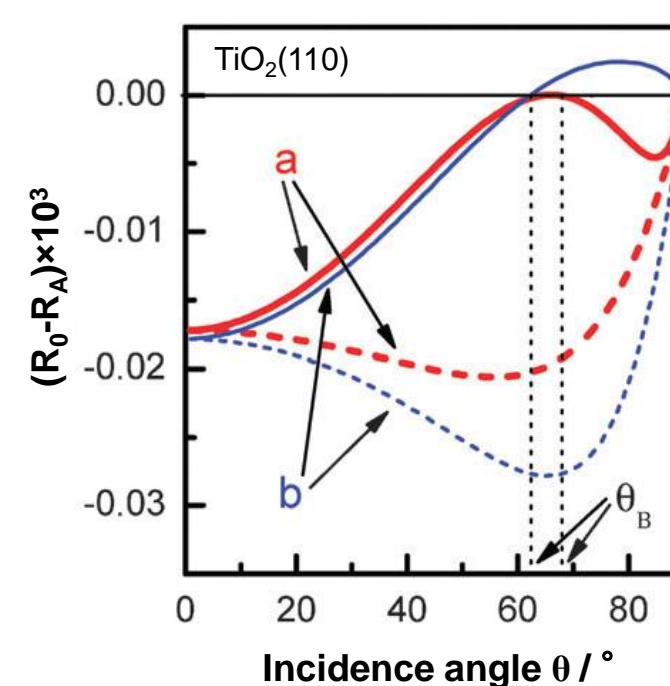


Figure 3. Calculated reflectivity differences between the clean $\text{TiO}_2(110)$ (R_0) and NO-covered $\text{TiO}_2(110)$ (R_A) as a function of incidence angle for p -polarized light (solid lines) and s -polarized light (dashed lines) at 1875 cm^{-1} . (a) oxidized $\text{TiO}_2(110)$, (b) reduced $\text{TiO}_2(110)$.⁵

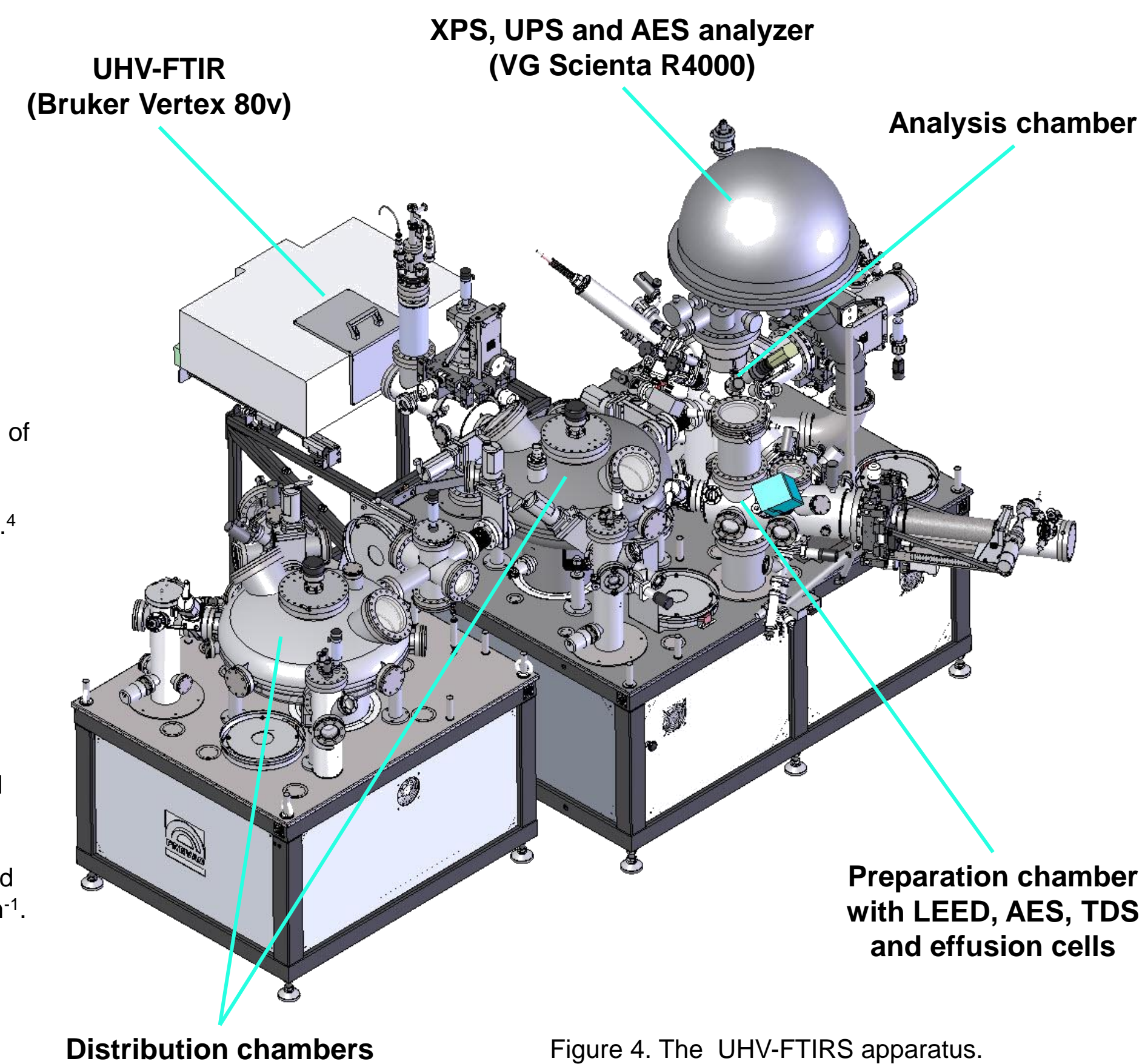


Figure 4. The UHV-FTIR apparatus.



Figure 5. Powder IR measurements in transmission mode

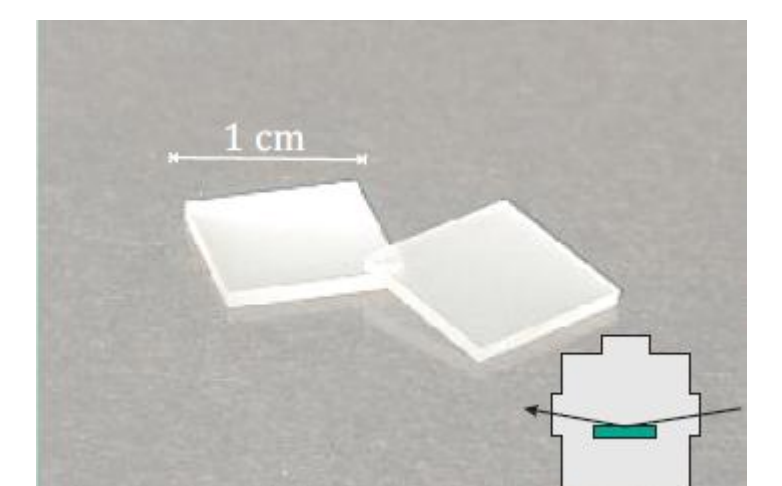


Figure 6. Oxide single crystals IR measurements in reflection mode

Carbon Monoxide on $\text{CeO}_2(111)$

Oxidized Surface

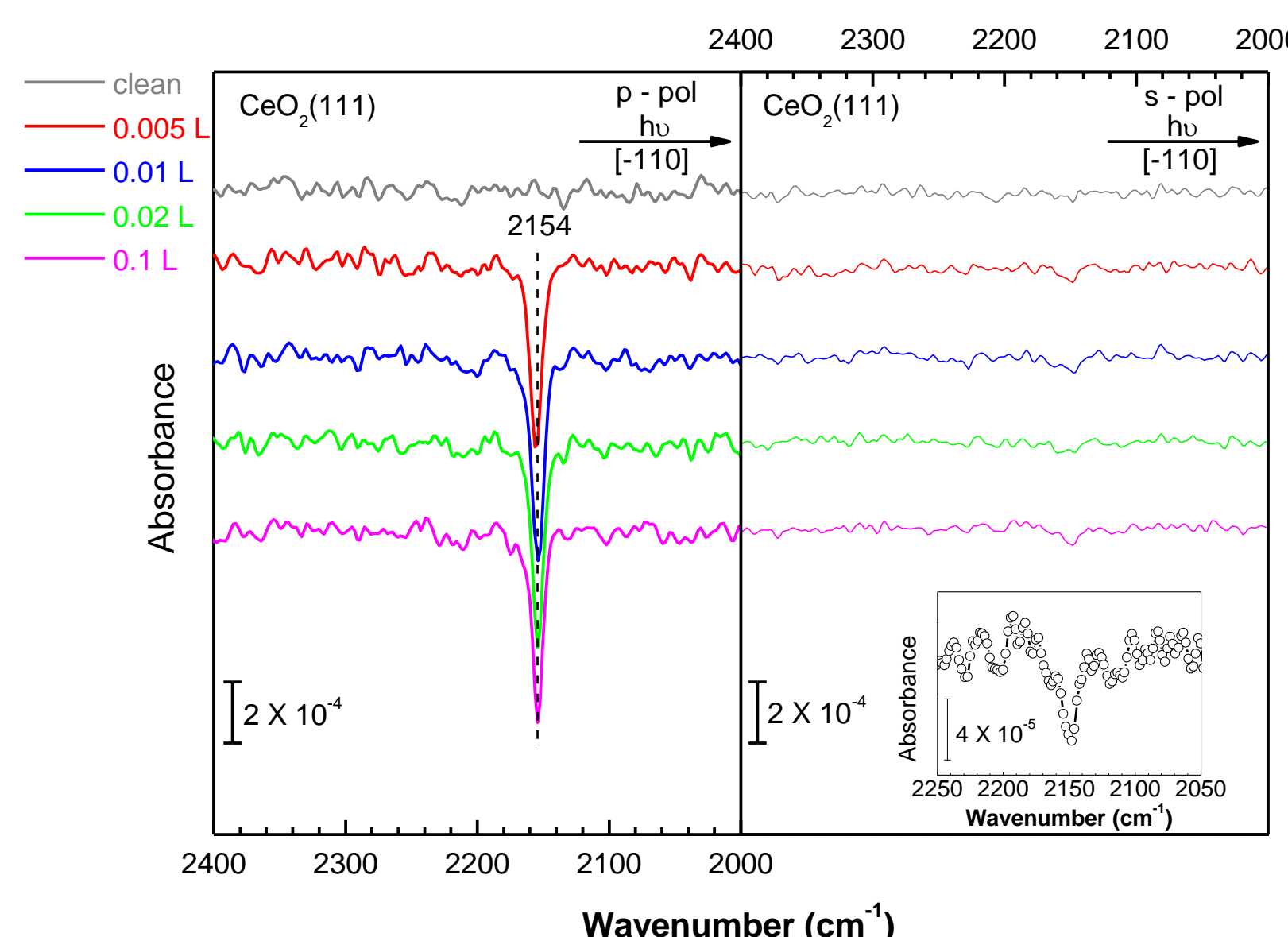


Figure 7. Experimental IRRAS spectra of different doses of CO at 68 K on oxidized $\text{CeO}_2(111)$ at a grazing incidence angle of 80° with (left) p - and (right) s -polarized light incident along $[-110]$. The inset shows a blow-up of the spectral region marked with an ellipse.

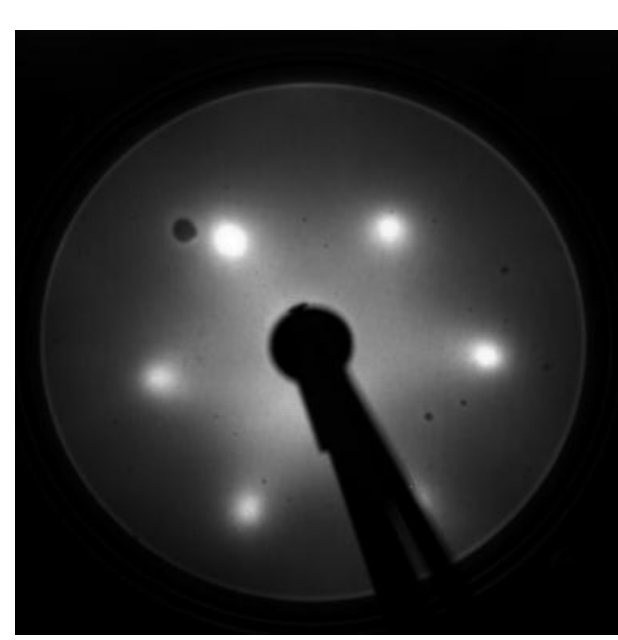


Figure 8. Low energy electron diffraction pattern from oxidized $\text{CeO}_2(111)$. Electron beam energy 70 eV.

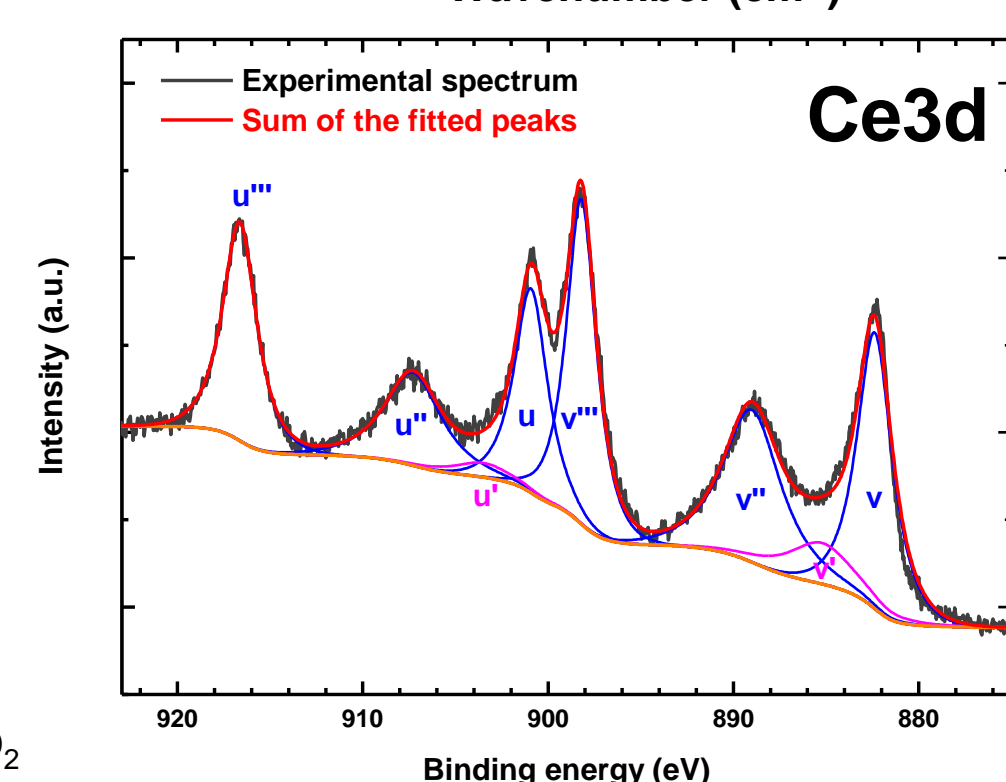


Figure 9. Fitted $\text{Ce}3d$ XPS spectrum of the oxidized $\text{CeO}_2(111)$.

- a sharp negative peak at 2154 cm^{-1} for p -polarization.
- only a very weak, also negative, feature for s -polarized light.
- this band can be assigned to CO molecules bound to Ce^{4+}_{7c} cations.
- sharp spots in the (1×1) LEED-pattern assure a well-defined surface crystallinity of the substrate.
- the density of oxygen vacancies (O_v) on the oxidized $\text{CeO}_2(111)$ surface determined from fitted $\text{Ce}3d$ XPS spectrum is only 1.7%.

Reduced Surface

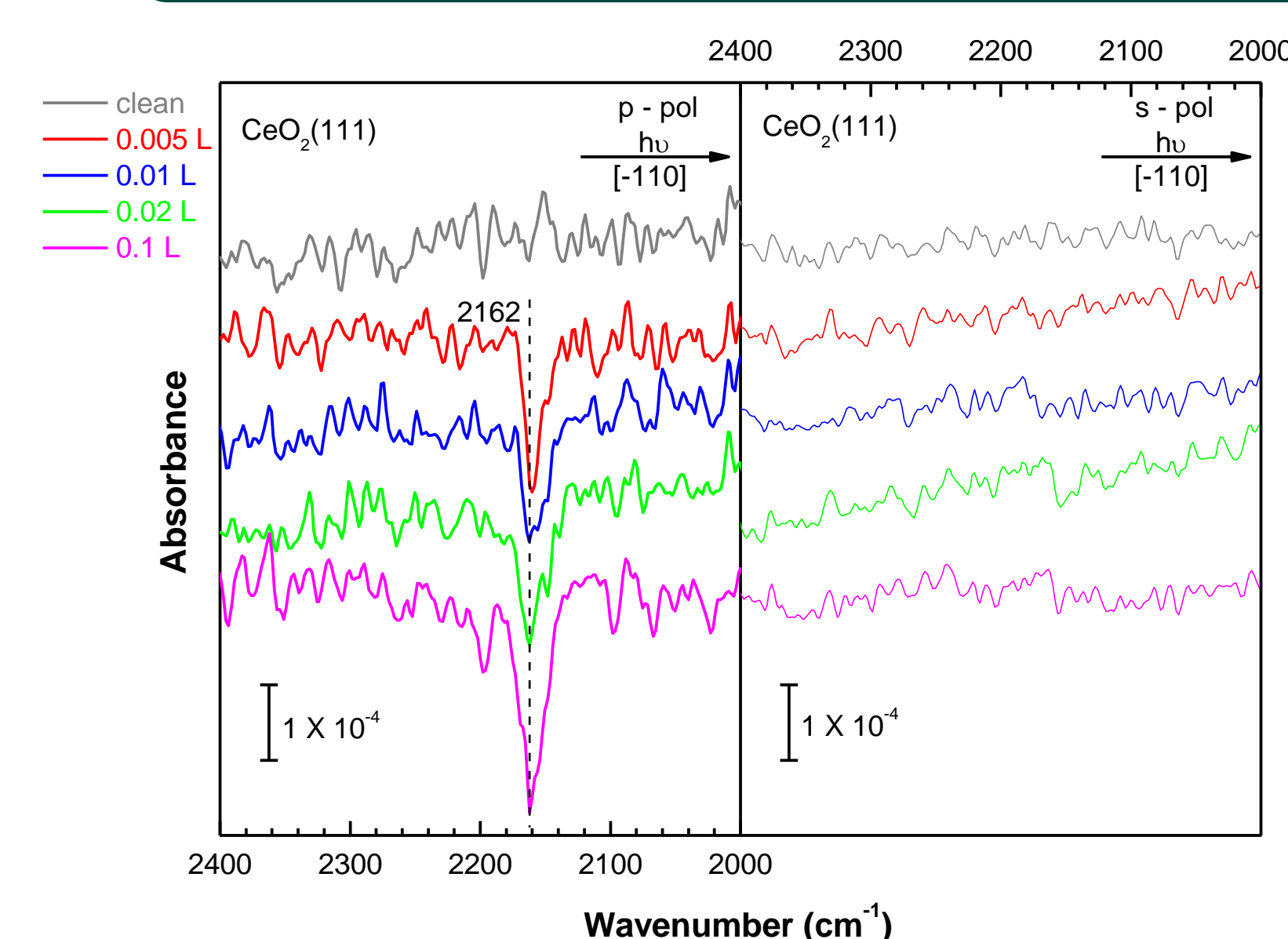


Figure 10. Experimental IRRAS spectra of different doses of CO at 74 K on reduced $\text{CeO}_2(111)$ at a grazing incidence angle of 80° with (left) p - and (right) s -polarized light incident along $[-110]$.

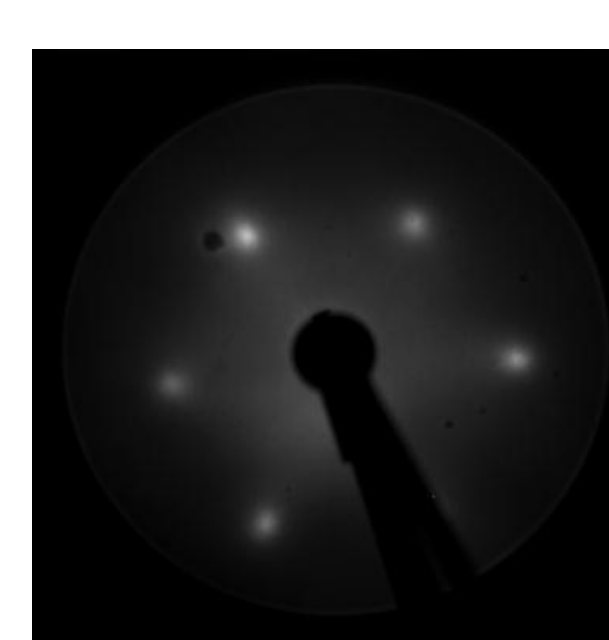


Figure 11. Low energy electron diffraction pattern from reduced $\text{CeO}_2(111)$. Electron beam energy 70 eV.

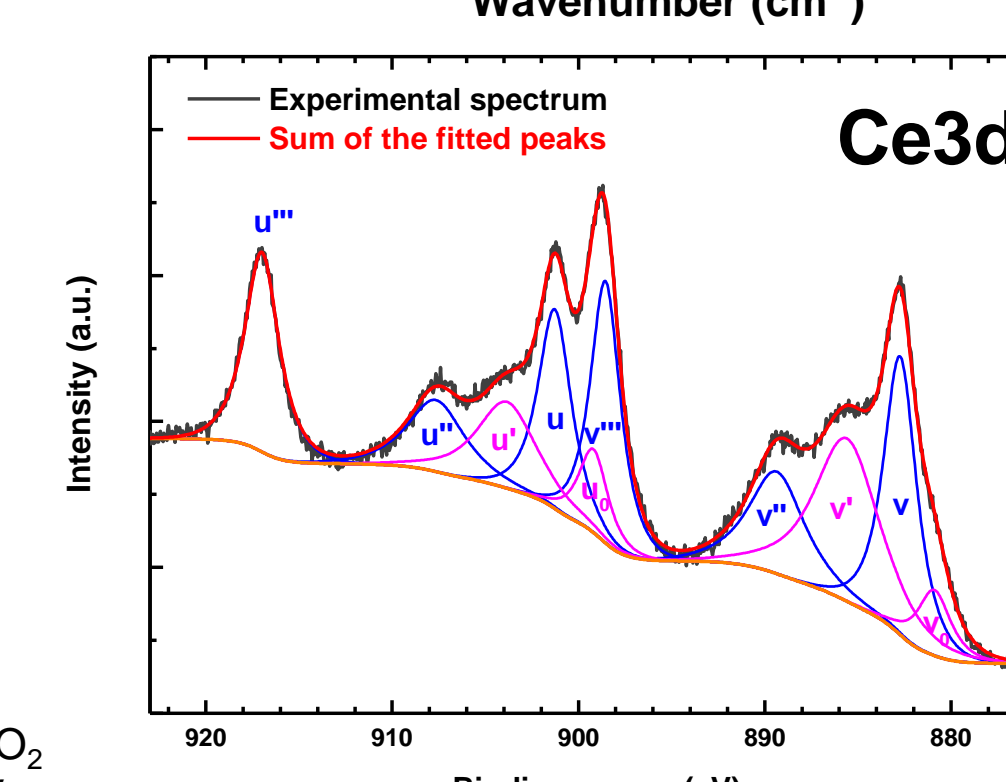


Figure 12. Fitted $\text{Ce}3d$ XPS spectrum of the reduced $\text{CeO}_2(111)$.

- the density of oxygen vacancies (O_v) deduced from fitted $\text{Ce}3d$ XPS spectrum is approximately 10%.
- a substantial broadening of the CO stretch peak, which is now centered at around 2162 cm^{-1} , for p -polarization.
- by applying a fitting procedure, we obtained a frequency of 2162 cm^{-1} for only one new species in addition to that observed at 2154 cm^{-1} for the clean surface.
- no visible feature for s -polarized light.
- surface crystallinity indicating by LEED.

Thermal Desorption

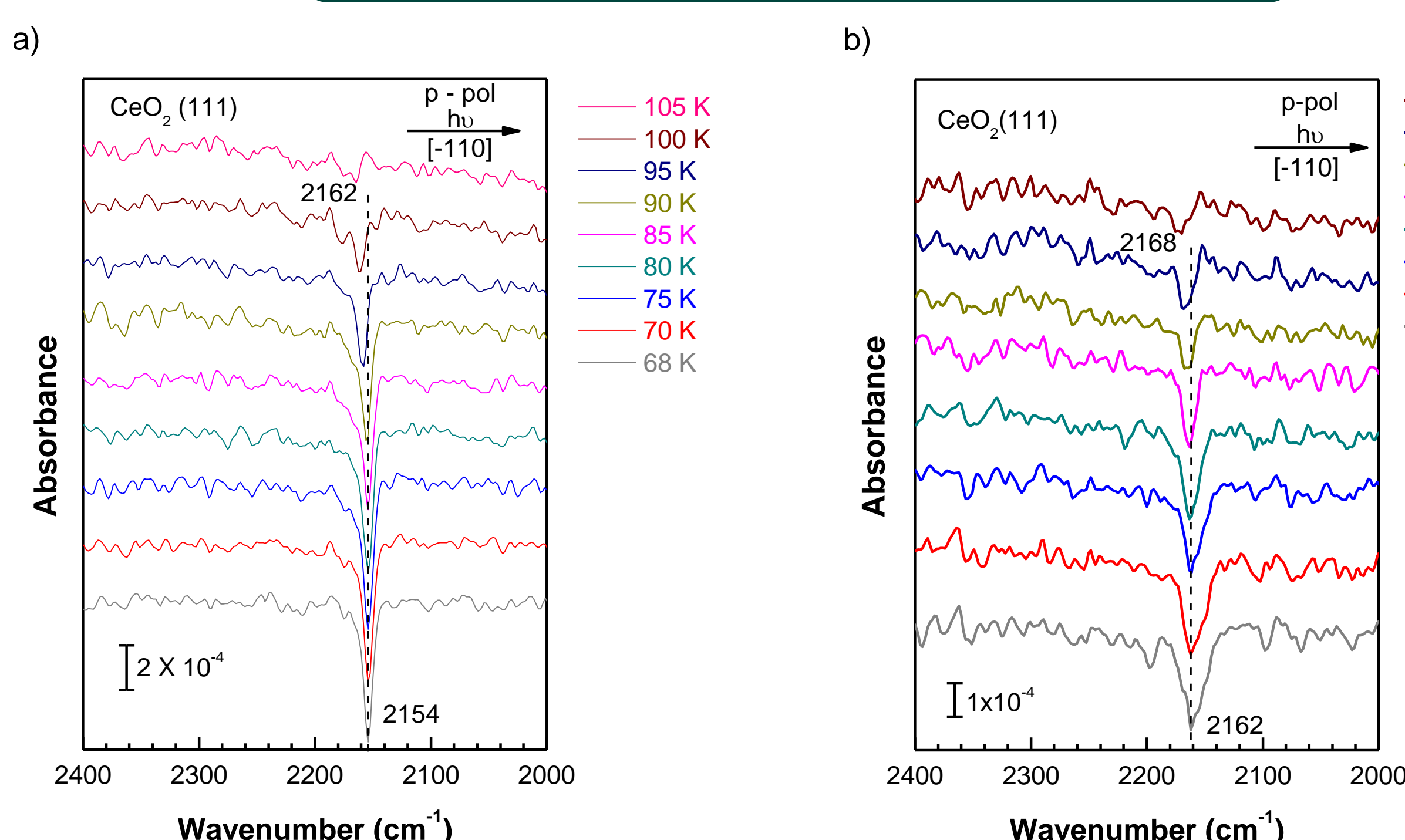


Figure 13. Experimental IRRAS spectra recorded directly after dosing of 0.1 L CO at ceria surfaces (lowest traces). The samples were gradually heated and spectra were recorded at the temperatures indicated. (a) CO on fully oxidized ceria surface, (b) CO on reduced surface.

Assignments of CO Bands

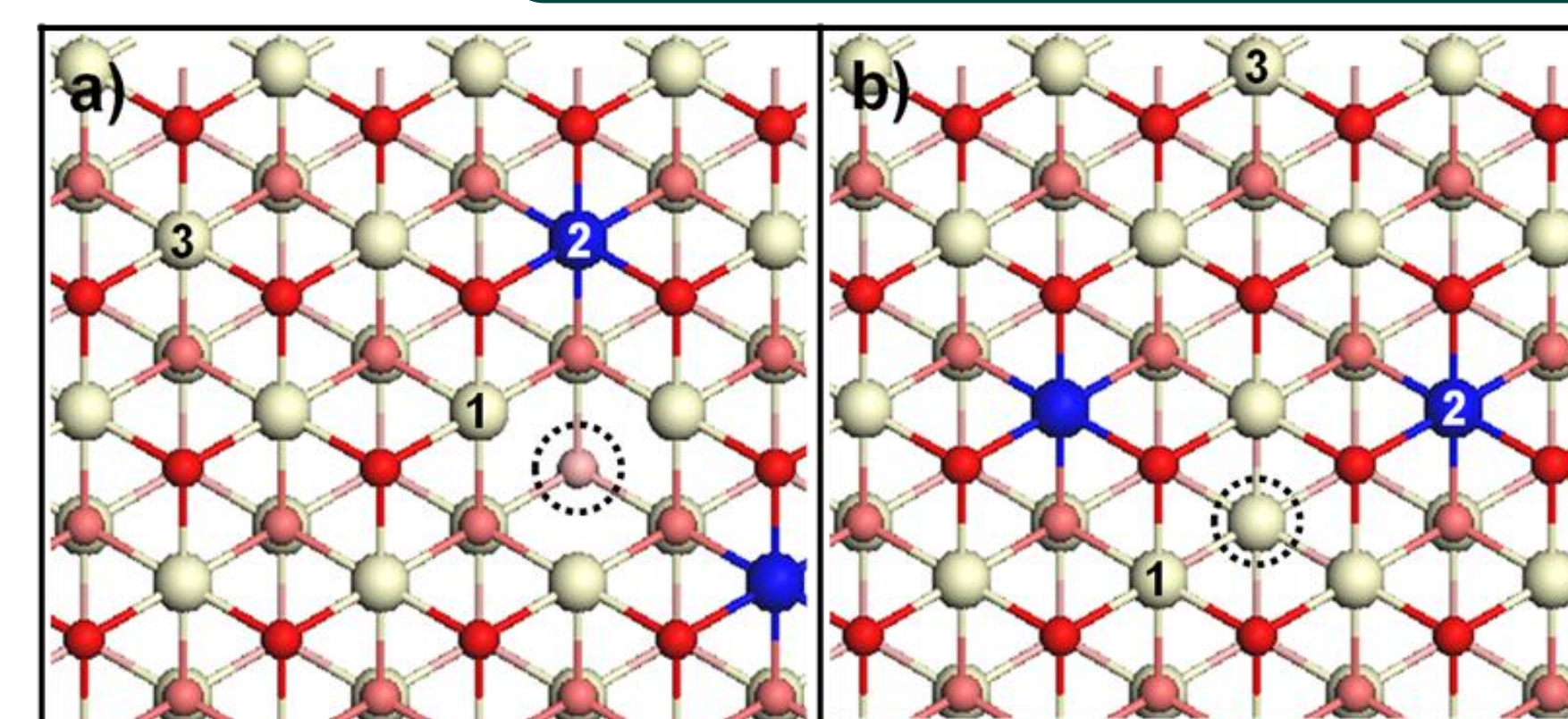


Figure 14. Ball-and-stick model of the $\text{CeO}_2(111)$ surface (top view) with (a) top- or (b) subsurface oxygen vacancy (V_O). Color: red - top surface oxygen, pink - subsurface oxygen, light red - 4th and 6th layer oxygen, white - Ce^{4+} , blue - Ce^{3+} .

- the band at 2154 cm^{-1} can be assigned to CO molecules bound to Ce^{4+}_{7c} cations (site 3 in Fig. 14).
- by systematic vdW-DFT+U calculations, we are able to assign the band shifted to 2162 cm^{-1} to CO adsorbed at Ce^{4+}_{6c} ions in the direct vicinity of the vacancy (site 1 in Fig. 14).

References

- [1] M. Xu, H. Noei, K. Fink, M. Muhler, Y. Wang and C. Wöll, *Angew. Chem. Int. Ed.*, **2012**, *51*, 4731-4734.
- [2] M. Xu, Y. Gao, E. M. Moreno, M. Kunst, M. Muhler, Y. Wang, H. Idriss and C. Wöll, *Phys. Rev. Lett.*, **2011**, *106*, 138302.
- [3] C. Yang, L. Yin, F. Bebensee, M. Buchholz, H. Sezen, S. Heissler, J. Chen, A. Nefedov, H. Idriss, X. Gong and C. Wöll, *PCCP*, **2014**, *16*, 24165.
- [4] J. Kattner and H. Hoffmann, *Handbook of Vibrational Spectroscopy*, John Wiley & Sons, Ltd, **2006**.
- [5] M. Xu, Y. Gao, Y. Wang and C. Wöll, *Phys. Chem. Chem. Phys.*, **2010**, *12*, 3649-3652.
- [6] M. V. Ganduglia-Pirovano, J. L. F. Da Silva and J. Sauer, *Phys. Rev. Lett.*, **2009**, *102*, 026101.

Acknowledgements

The authors would like to gratefully acknowledge the Helmholtz Research School Energy-Related Catalysis for financial support.